
This is an electronic reprint of the original article.

This reprint may differ from the original in pagination and typographic detail.

Author(s): Kivinen, P. & Savin, A. & Zgirski, M. & Törmä, P. & Pekola, Jukka & Prunnila, M. & Ahopelto, J.

Title: Electron phonon heat transport and electronic thermal conductivity in heavily doped silicon-on-insulator film

Year: 2003

Version: Final published version

Please cite the original version:

Kivinen, P. & Savin, A. & Zgirski, M. & Törmä, P. & Pekola, Jukka & Prunnila, M. & Ahopelto, J. 2003. Electron phonon heat transport and electronic thermal conductivity in heavily doped silicon-on-insulator film. *Journal of Applied Physics*. Volume 94, Issue 5. 3201-3205. ISSN 0021-8979 (printed). DOI: 10.1063/1.1592627.

Rights: © 2003 American Institute of Physics. This article may be downloaded for personal use only. Any other use requires prior permission of the author and the American Institute of Physics. The following article appeared in *Journal of Applied Physics*, Volume 94, Issue 5 and may be found at <http://scitation.aip.org/content/aip/journal/jap/94/5/10.1063/1.1592627>

Electron–phonon heat transport and electronic thermal conductivity in heavily doped silicon-on-insulator film

P. Kivinen, A. Savin, M. Zgirski, P. Törmä, J. Pekola, M. Prunnila, and J. Ahopelto

Citation: [Journal of Applied Physics](#) **94**, 3201 (2003); doi: 10.1063/1.1592627

View online: <http://dx.doi.org/10.1063/1.1592627>

View Table of Contents: <http://scitation.aip.org/content/aip/journal/jap/94/5?ver=pdfcov>

Published by the [AIP Publishing](#)

Articles you may be interested in

[Self-consistent calculations of inversion-layer mobility in highly doped silicon-on-insulator metal–oxide–semiconductor field-effect transistors](#)

[J. Appl. Phys.](#) **90**, 866 (2001); 10.1063/1.1378329

[Asymmetrical heating behavior of doped Si channels in bulk silicon and in silicon-on-insulator under high current stress](#)

[J. Appl. Phys.](#) **86**, 6895 (1999); 10.1063/1.371769

[Dopant activation of heavily doped silicon-on-insulator by high density currents](#)

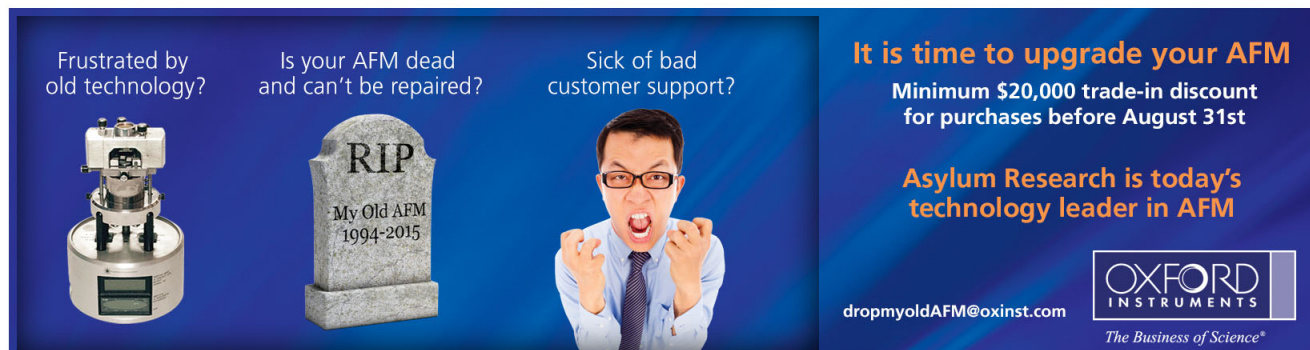
[J. Appl. Phys.](#) **86**, 1552 (1999); 10.1063/1.370928

[Phonon-limited electron mobility in ultrathin silicon-on-insulator inversion layers](#)

[J. Appl. Phys.](#) **83**, 4802 (1998); 10.1063/1.367273

[Single-electron transistors fabricated from a doped-Si film in a silicon-on-insulator substrate](#)

[Appl. Phys. Lett.](#) **72**, 795 (1998); 10.1063/1.120896

An advertisement for Oxford Instruments' Asylum Research AFM technology. The background is dark blue. On the left, there is a photograph of an AFM head. In the center, there is a grey tombstone with the inscription 'RIP My Old AFM 1994-2015'. To the right of the tombstone is a photograph of a man in a white shirt and tie, looking frustrated with his hands raised. Text on the left side reads: 'Frustrated by old technology?', 'Is your AFM dead and can't be repaired?', and 'Sick of bad customer support?'. On the right side, the text reads: 'It is time to upgrade your AFM', 'Minimum \$20,000 trade-in discount for purchases before August 31st', and 'Asylum Research is today's technology leader in AFM'. At the bottom right, the Oxford Instruments logo is shown with the tagline 'The Business of Science®'. Below the logo, the email address 'dropmyoldAFM@oxinst.com' is provided.

Electron–phonon heat transport and electronic thermal conductivity in heavily doped silicon-on-insulator film

P. Kivinen,^{a)} A. Savin, M. Zgirska, and P. Törmä

Department of Physics, University of Jyväskylä, P.O. Box 35, FIN-40014 Jyväskylä, Finland

J. Pekola

Low Temperature Laboratory, Helsinki University of Technology, P.O. Box 2200, 02015 HUT Helsinki, Finland

M. Prunnila and J. Ahopelto

VTT Center for Microelectronics, P.O. Box 1101, FIN-2044 VTT, Finland

(Received 4 March 2003; accepted 27 May 2003)

Electron–phonon interaction and electronic thermal conductivity have been investigated in heavily doped silicon at subKelvin temperatures. The heat flow between electron and phonon systems is found to be proportional to T^6 . Utilization of a superconductor–semiconductor–superconductor thermometer enables a precise measurement of electron and substrate temperatures. The electronic thermal conductivity is consistent with the Wiedemann–Franz law. © 2003 American Institute of Physics. [DOI: 10.1063/1.1592627]

INTRODUCTION

Investigation of the heat transport processes in heavily doped silicon at low temperature is important both for developing various low temperature devices such as hot electron bolometers¹ or microcoolers² and also for fundamental physics. Electron–phonon interaction is very weak at low temperature and this leads to a large temperature difference between electron and phonon systems even when a relatively small power is introduced into the system. Therefore hot electron effects can impose constraints on electronic devices and one has to take into account the power consumption per unit volume. Electron–phonon interaction, or more specifically electron–phonon relaxation time τ_{e-ph} in pure metals is inversely proportional to the number of thermal phonons³ and therefore $\tau_{e-ph}^{-1} \propto T^3$ for three dimensional (3D) phonons. This dependence is experimentally and theoretically well established (see e.g., Refs. 4 and 5). The situation becomes more complicated when material is disordered. Electron scattering from impurities and boundaries significantly changes the single-particle picture of electron–phonon interaction. Two scattering processes should be taken into account: the “pure” electron–phonon scattering, which is the only electron–phonon interaction mechanism in pure metals, and the inelastic electron scattering from impurities such as defects or boundaries. Depending on the product of thermal phonon wave vector q_T and electron mean free path l , one can consider two marginal cases for electron–phonon interaction: clean ($q_T l \gg 1$) and dirty ($q_T l \ll 1$) limits. Phenomenologically this means that in dirty limit electrons scatter mostly from impurities or defects and in clean limit the dominating scattering is from phonons, but impurities and defects do not play a significant role.

The electron–phonon interaction has been intensively investigated experimentally^{3,4,6–26} and theoretically.^{5,27–29} Experimental results confirm $\tau_{e-ph}^{-1} \propto T^3$ dependence in pure metals,^{4,6–11} as well as in metal–oxide–semiconductor field-effect-transistors (MOSFETs)¹² and in various heterostructures.^{13–15} Some of the experimental results^{3,14,16–24} report T^2 and T^4 dependencies for τ_{e-ph}^{-1} . This discrepancy of the T dependence can be described by the sensitivity of the electron–phonon interaction in dirty limit to the microscopic parameters of the sample. In the presence of the static scattering potential, $\tau_{e-ph}^{-1} \propto T^2$ is expected.²⁷ J.J. Lin¹⁶ and Lin and Wu¹⁷ observed $\tau_{e-ph}^{-1} \propto T^2$ for disordered dilute $\text{Ti}_{1-x}\text{Al}_x$ samples. Bergmann *et al.*¹⁸ reported the same behavior for thin gold film on quartz, Smith and Wybourne¹⁹ for free-standing AuPd wires, Chow *et al.*¹⁴ for 2D electron gas in $\text{GaAs}/\text{Al}_x\text{Ga}_{1-x}\text{As}$ heterostructure, DiTusa *et al.*²⁰ for CuCr films, and Pitsina *et al.*²¹ for Au, Al, Be, Nb, and NbC films. This T^2 behavior can be partly explained by the scattering from the static potential, but this is not the case, e.g., in thin gold film.¹⁸ If the impurities are fully vibrating with the lattice, which is the case in heavily doped silicon, the relaxation rate is proportional to T^4 : $\tau_{e-ph}^{-1} \propto T^4 l$,^{27,28} where l is the electron mean free path. This behavior in dirty limit has been derived by Thouless²⁹ and Reizer.⁵ Gershenson *et al.*²² reported a T^4 dependence for τ_{e-ph}^{-1} in ultrathin Hf and Ti samples at milliKelvin temperatures. They also observed the suppression of electron–phonon interaction by disorder. Wu *et al.*²³ observed a T^4 behavior in $\text{Ti}_{1-x}\text{Ge}_x$ samples, Komnik *et al.*³ in thin Bi films, and Heslinga and Klapwijk²⁴ in n -type silicon in the temperature range 1.2–4.8 K.

The electron–phonon heat transport in the heavily doped silicon-on-insulator (SOI) film has been investigated in our work at subKelvin temperatures. In the case of silicon, which is heavily doped with phosphorous ($4.0 \times 10^{19} \text{ cm}^{-3}$), the electron mean free path l at subkelvin temperature is about

^{a)} Author to whom correspondence should be addressed; electronic mail: pasi.kivinen@phys.jyu.fi

5 nm²⁴ and velocity of sound $v_s = 5000$ m/s. Taking into account that the phonon wave vector $q_T = k_b T / \hbar v_s$ we obtain $q_T l = (0.13)T$, where T is temperature in Kelvin. This indicates that the electron–phonon processes in our case are well within the disorder limit at subkelvin temperatures ($q_T l \ll 1$).

The dimensionality of the phonon distribution at low temperature may differ from 3D in thin films which affects the temperature dependence of τ_{e-ph} . The phonon wavelength depends on temperature, and when the film thickness is of the same order of magnitude as the phonon wavelength, the dimensionality of the phonon system changes.³⁰ The acoustic mismatch between the film and the substrate also affects the dimensionality of the phonons in the film. Generally a good coupling between the phonons in the substrate and in the film eliminates the low dimensionality effect. The thickness of the SOI film investigated in this work was 70 nm. The possible acoustic mismatch is negligible between heavily doped silicon and SiO₂ due to the acoustic similarity of these materials and it is reasonable to assume that electrons interact with 3D phonons. Heavily doped Si investigated in the present work is in the dirty limit at subKelvin temperature and the phonon system has a complete phonon drag, therefore according to the theory^{5,27,29} the electron–phonon interaction relaxation time τ_{e-ph}^{-1} is supposed to be proportional to T^4 .

SAMPLES AND THERMOMETRY

The widths of the SOI films under investigation were 30–60 μm and the length of the films exceeded 1500 μm . The thickness of the film was 70 nm and the electron concentration was $4.0 \times 10^{19} \text{ cm}^{-3}$. The thickness of thermal oxide on top of the SOI film and the buried oxide layer was 68 and 400 nm, respectively. At 4.2 K the resistivity of the film was 1.04 m Ω cm and the Fermi level given by the free electron formula is $E_f \approx 40$ meV. The electron mean free path in heavily doped silicon is $l \approx 5$ nm.²⁴ The sample fabrication has already been described in detail elsewhere.³¹ The measurements were performed in a ³He/⁴He dilution refrigerator.

The electrons in the SOI film were heated above the lattice temperature by electric current. The electron temperature was measured by superconductor–semiconductor (heavily doped Si)–superconductor (S–Sm–S) junctions, which were calibrated against the RuO thermometer mounted on the copper sample holder. In the S–Sm–S structure the quasiparticle tunneling across the junction is sensitive to the electron temperature. The current–voltage characteristics of the S–Sm–S structure with two $3 \times 3 \mu\text{m}^2$ junctions are shown in Fig. 1(a). They exhibit strong temperature dependence below the critical temperature of the superconductor. When the S–Sm–S structure is biased with constant current I_0 [see inset in Fig. 1(b)] the voltage over the junctions is a function of the electron temperature in the silicon film [see Fig. 1(b)]. The bias current I_0 was few orders of magnitude smaller than the current used for the electron heating in the Si film and therefore the possible heating by the bias current can be neglected.

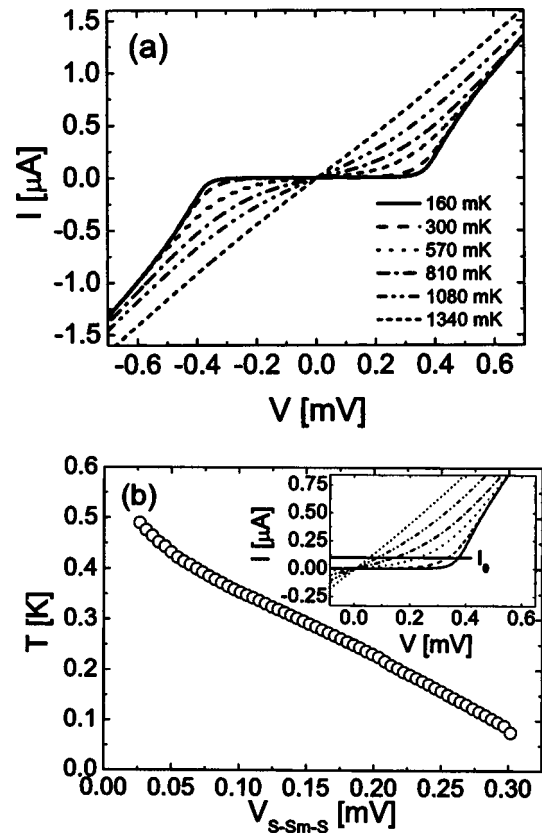


FIG. 1. (a) Current–voltage (I – V) characteristics of a $3 \times 3 \mu\text{m}^2$ S–Sm–S structure at different temperatures. (b) S–Sm–S thermometer calibration curve ($3 \times 3 \mu\text{m}^2$ junctions), biased by a constant current I_0 . (Inset) I – V characteristics and the bias current in the temperature measurement.

ELECTRON–PHONON INTERACTION

At low temperature we consider electrons having a well-defined temperature, because the electron–electron interaction time (τ_{e-e}) is supposed to be significantly smaller than the electron–phonon interaction time (τ_{e-ph}). The heat flow from electrons to phonons can be described by a model,¹⁵ where electrons have heat capacity $C_e = \gamma T_e$ and the change of the electron temperature is determined by $dP = \tau_{e-ph}^{-1} C_e dT_e$. By substituting $\tau_{e-ph}^{-1} = \alpha T^p$, we obtain

$$P = \Sigma \Omega (T_e^{p+2} - T_{ph}^{p+2}), \quad (1)$$

where P is the heat flow from electrons to phonons, Σ is a material-dependent constant characterizing the electron–phonon coupling: $\Sigma = \alpha \gamma / (p+2)$, Ω is the volume, and T_e (T_{ph}) is the electron (phonon) temperature.

The measurements of the electron–phonon coupling constant in SOI films have been done at substrate temperature between 100 and 500 mK. The heating current was swept slowly and the electron and phonon (actually temperature of the silicon bar near to the sample, see Fig. 2) temperatures were measured simultaneously. In our experiment an additional S–Sm–S thermometer, which was electrically isolated from the silicon film, was placed near the Si film (see Fig. 2). Below 1 K the electron–phonon thermal resistance in silicon is considerably larger than the Kapitza resistance between the silicon film and the silicon oxide layer, and therefore the S–Sm–S thermometer next to the silicon

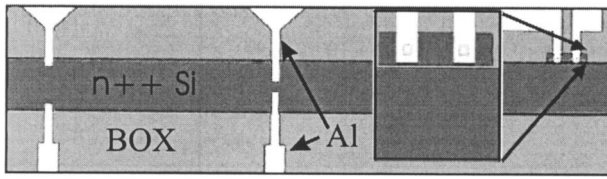


FIG. 2. Micrograph of the sample for the electron-phonon coupling measurement. The horizontal dark bar is the SOI film (width $60\ \mu\text{m}$) and the white vertical bars are aluminum contacts, which are used for the temperature measurement. (Inset) The phonon thermometer is an electrically isolated small SOI bar with two aluminum contacts.

film is assumed to be at approximately the same temperature as the phonon system in the silicon film.

The electron and phonon temperatures as functions of the heating power are plotted in Fig. 3(a). The bath temperature is $168\ \text{mK}$. At power density of $1 \times 10^5\ \text{W/m}^3$ the electron temperature is about twice above the bath temperature. Experimental $P(T_{\text{el}})$ dependence well corresponds to the theoretical behavior [Eq. (1)] with $p=3$ if we assume $T_{\text{ph}} = T_{\text{bath}} = \text{const.}$ ^{31,32} However, it can be seen from Fig. 3 that the phonon system in the SOI film is overheated and the increase of phonon temperature is comparable to the change of the electron temperature in the most of the heating range.

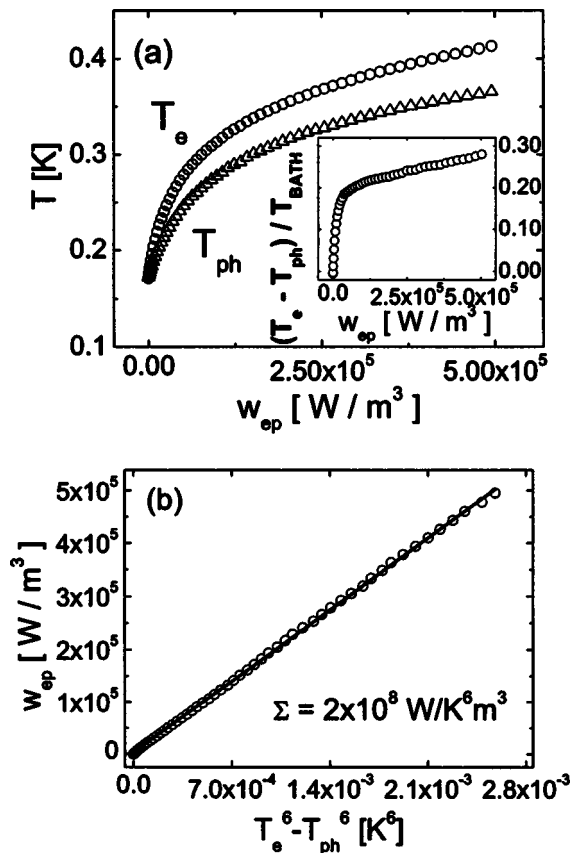


FIG. 3. (a) The electron (T_e) and phonon (T_{ph}) temperatures as a function of the applied power density at $T_{\text{bath}} = 168\ \text{mK}$. Electron and phonon systems are strongly overheated, the temperature difference between them scaled by substrate temperature is presented in inset. (b) The applied power density is plotted against $(T_e^6 - T_{\text{ph}}^6)$. The value of the electron-phonon coupling constant Σ derived from the linear fit (solid line) by equation 1 is $\Sigma = 2 \times 10^8\ \text{W/K}^6\ \text{m}^3$.

Therefore we cannot consider the phonon temperature to be constant and equal to the bath temperature. The heating power density is plotted against $(T_e^6 - T_{\text{ph}}^6)$ in Fig. 3(b). The dependence is linear in this scale and it indicates that the heat flow between the electron and phonon systems has a T^6 dependence. This corresponds to $\tau_{e-\text{ph}}^{-1} \propto T^4$ for the electron-phonon interaction relaxation time or in other words the microscopic dimensionality parameter p in Eq. (1) equals 4. This result is in agreement with the theoretical result for dirty systems with full phonon drag of ionized impurities.^{5,29} The Σ derived from the data presented in Fig. 3(b) is $2 \times 10^8\ \text{W/K}^6\ \text{m}^3$. If we compare this value with recent experimental values for thin Hf films,²² we find that α in our case is at least 2 orders of magnitude higher. However, the electron-phonon coupling, which is characterized by Σ , is actually the same order of magnitude. This is due to significantly smaller electron density in our doped Si samples compared with Hf.

ELECTRON THERMAL CONDUCTIVITY

Thermal conductivity in degenerate silicon at low temperature is an essential issue in the design of nanoscale devices. At low temperature the electron thermal conductivity often determines the heat transport. According to the Wiedemann-Franz law, the ratio of thermal and electrical conductivities is proportional to temperature and the constant of proportionality is called the Lorenz number L , whose theoretical value is $L_0 \approx 2.44 \times 10^{-8}\ \text{W/K}^2$. This is the case, when the electron gas is highly degenerate and the electron mean free path is the same for electrical and thermal conductivities. Deviation from the theoretical value L_0 may have several origins. The impurities, presence of magnons, and phonon contribution to thermal conductivity affect the value of the Lorenz number.³³ Generally the Wiedemann-Franz law is valid for degenerate semiconductors at low temperature. Syme *et al.*³⁴ measured the electronic thermal conductivity in a two-dimensional electron gas in n -channel MOSFETs at low temperature ($1\text{--}10\ \text{K}$) and the measured temperature dependence of the electronic thermal conductivity was in agreement with the Wiedemann-Franz law.

The results of our electron-phonon heat transport measurements in SOI films allow us to estimate the electronic thermal conductivity from the nonuniform heating experiments. The data reported above can be used for calculation of the heat flow between electron and phonon systems and provide information about contribution of the electronic thermal conductivity in thermal transport. Contrary to the electron-phonon coupling the temperature gradient along the SOI film is the essential condition for the electronic thermal conductivity measurement. In a steady state the heat flow in the electron system can be determined by the thermal conductivity along the silicon bar and by the energy flow rate between electrons and phonons³⁴

$$\frac{d}{dx} \left(\kappa(T) \cdot \frac{dT}{dx} \right) = w_{\text{ep}}(T), \quad (2)$$

where $\kappa(T)$ is the electron thermal conductivity and w_{ep} is power density $P_{e-\text{ph}}/\Omega$, i.e., heat flow between electron and

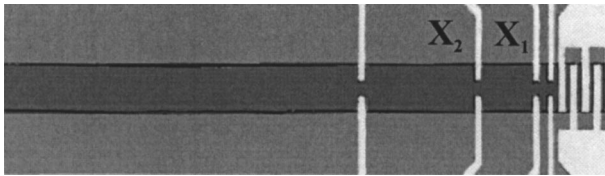


FIG. 4. Micrograph of the SOI film used in the electron thermal conductivity measurements. The horizontal dark silicon bar (width 30 μm), was heated at the right end. Several pairs of vertical aluminum contacts were used for the electron temperature measurement along the bar. An extra thermometer (not seen in the figure) was used to control the temperature of the silicon bar far from the heater.

phonon systems per unit volume. If we assume validity of the Wiedemann–Franz law, the electron thermal conductivity can be presented in the form

$$\kappa = L\sigma T, \quad (3)$$

where σ is the electrical conductivity. Taking into account the linear temperature dependence of electron thermal conductivity, Eq. (2) can be presented in the form

$$\begin{aligned} T \cdot \frac{dT}{dx} &= - \left[\int_{T_{\text{bath}}}^T 2 \cdot (\sigma \cdot L)^{-1} \cdot w_{\text{ep}}(u) \cdot u \cdot du \right]^{1/2} \\ &= - \sqrt{\frac{2}{\sigma \cdot L}} \cdot [I_1(T)]^{1/2}, \end{aligned} \quad (4)$$

and finally, taking into account boundary conditions for a very long sample

$$(x_2 - x_1) \cdot \sqrt{\frac{2}{\sigma \cdot L}} = \int_{T_2}^{T_1} \frac{T \cdot dT}{[I_1(T)]^{1/2}} = I_2(T_1, T_2), \quad (5)$$

where $(x_2 - x_1)$ is the distance between two points along the bar and T_1 and T_2 are the corresponding electron temperatures. In other words integral I_2 on the right side depends only on the distance between two points along the bar. For the two fixed points x_1 and x_2 the value of the integral is constant in the whole range of the power applied to the system. This is valid only for very long samples and moderate energy flow in the system.

The sample used for the measurement is depicted in Fig. 4. The silicon bar was 30 μm wide and S–Sm–S thermometers T_1 and T_2 used for the measurement were placed 40 μm apart. To obtain the temperature profile along the silicon film, one usually measures the electron temperature in several points along the line. In our experiment we used only two S–Sm–S thermometers for measuring temperature gradient along the sample, and one thermometer at the “cold” end of the sample. The heating power was slowly swept and the electron temperature in two points along the bar (T_1 and T_2) was recorded. If we suggest that the temperature T_2 is determined only by temperature T_1 (very long sample), using these data we can plot the model temperature decay along the bar (see Fig. 5): the circles are the measured electron temperature values and the solid line corresponds to the analytical solution of Eq. (2). The only fitting parameter is the Lorenz number L , which is $2.45 \times 10^{-8} \text{ W } \Omega \text{ K}^{-2}$. The result of the fitting may be considered as rather good, but the actual deviation of the calculated $(T_e - T_{\text{bath}})$ from experimen-

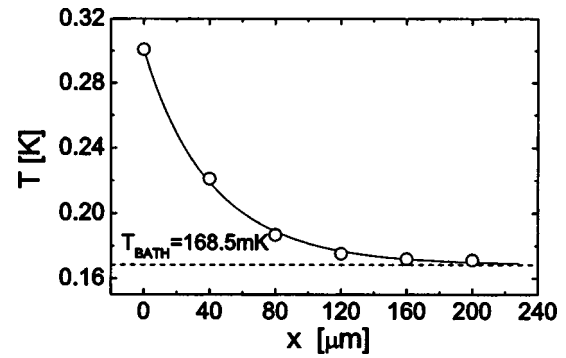


FIG. 5. Electron temperature profile along the sample (circles) represent experimental data. The solid line is the fitting with Eq. (2) (the Lorenz number obtained from the fitting is $L = 2.45 \times 10^{-8} \text{ W } \Omega / \text{K}^2$). The dashed line corresponds to the bath temperature 168.5 mK.

tal data is rather large for large x values. As we demonstrate below, the analysis based on the electron temperature measurements in two points along the bar as a function of power applied to the electron system and the calculation of the integral from Eq. (5) is more sensitive to any deviation from the Wiedemann–Franz law. The temperature of the S–Sm–S thermometer T_2 situated in point x_2 (see Fig. 4) is plotted as a function of T_1 in Fig. 6(a). The Lorenz number L , which was calculated from this dependence on the basis of Eq. (5) [in Eq. (5) the integral on the right side depends only on the two temperatures T_1 and T_2], is plotted as a function of the electron temperature T_1 in Fig. 6(b). The Lorenz number slightly increases with the increase of the heating power at $T_1 < 2T_{\text{sub}}$ and demonstrates very rapid growth when the electron temperature exceeds the substrate one by a factor of 2.

In calculating the value of the Lorenz number we assume that the phonons in the silicon film are similarly heated as in the electron–phonon interaction measurement, but this assumption might be incorrect. The phonon contribution to the thermal conductivity leads to an increase of the Lorenz number derived from Eq. (5). Parallel heat conductivity in substrate is probably responsible for the observed increase of the Lorenz number. The heat flow in the phonon system

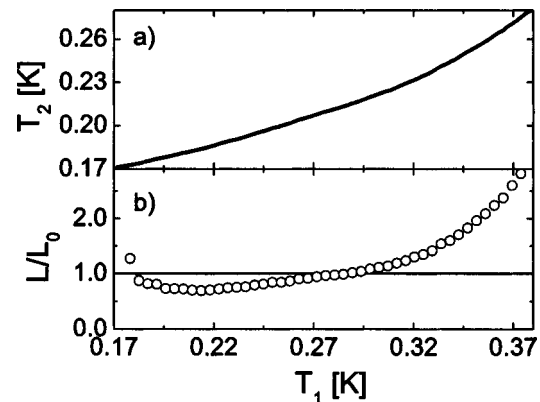


FIG. 6. (a) The electron temperature T_2 plotted against T_1 (see Fig. 4). The thermometers are placed 40 μm apart and the bath temperature is 168.5 mK. (b) The relative Lorenz number as a function of electron temperature T_1 .

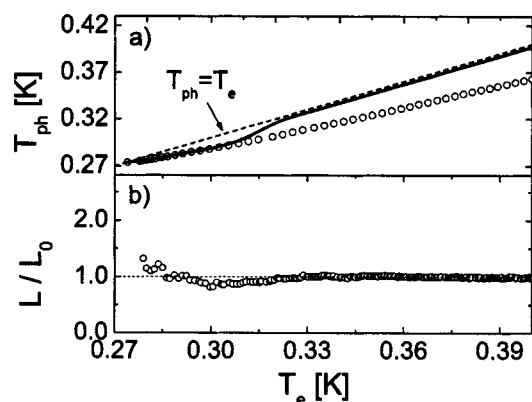


FIG. 7. (a) Phonon temperature in the SOI film in the case of uniform heating of the film as a function of the electron temperature (open circles) and that from the model used to analyze the electron heat conductance experiment (solid line). (b) The Lorenz number calculated by taking into account the predicted phonon temperature profile.

leads to an additional increase of the phonon temperature and to a decrease of the heat flow from the electron system and the value of I_1 [see Eqs. (1) and (4)].

The circles in Fig. 7(a) represent the phonon temperature in the electron–phonon interaction experiment as a function of the electron temperature and correspond to a uniform heating of the SOI film. The solid line is the model temperature dependence for the phonon overheated due to a parallel thermal conductivity. By introducing the parallel heat conduction model the situation is improved (see Fig. 7(b)). Integral I_1 is calculated using T_e and T_{ph} from the electron–phonon coupling measurement for the low temperature range, but above 300 mK a higher value of the phonon temperature is used for calculations. In the temperature range below 300 mK phonons are overheated above the substrate temperature in the same manner as in the electron–phonon interaction measurement and we can neglect the effect of the phonon thermal conductance. At higher temperature phonon system is heated more strongly and the phonon temperature approaches the electron temperature. Physically this means that the parallel heat conductivity of the phonon systems in substrate and in the SOI film starts to dominate in the heat transfer process at higher temperature. By this assumption an agreement with the Wiedemann–Franz law is achieved.

CONCLUSIONS

Heat transport properties of the electron system in degenerate *n*-type silicon have been studied. The lattice in heavily doped silicon film is heated above the substrate temperature, which must be taken into account in the analysis. The heat flow between electron and phonon systems demonstrates a T^6 dependence, which is in accordance with the theoretical prediction for a dirty system. The electron thermal conductivity dominates at low temperature and parallel heat conduction in the phonon system must be taken into account at temperatures above 300 mK. Taking into account

the phonon overheating in the SOI film due to parallel heat conduction drastically improves the agreement of the experimental data with the Wiedemann–Franz law.

ACKNOWLEDGMENTS

This work has been supported by the Academy of Finland under the Finnish Center of Excellence Project No. 2000-2005 (Project No. 44875, Nuclear and Condensed Matter Program at JYFL) and by Vilho, Yrjö and Kalle Väisälä Foundation.

- ¹D. V. Anghel, A. Luukanen, and J. P. Pekola, *Appl. Phys. Lett.* **78**, 556 (2001).
- ²A. J. Manninen, J. K. Suoknuuti, M. M. Leivo, and J. P. Pekola, *Appl. Phys. Lett.* **74**, 3020 (1999).
- ³Yu. F. Komnik, V. Yu. Kashrin, B. I. Belevtsev, and E. Yu. Beliaev, *Phys. Rev. B* **50**, 15298 (1994).
- ⁴P. Santhanam and D. E. Prober, *Phys. Rev. B* **29**, 3733 (1984).
- ⁵M. Yu. Reizer, *Phys. Rev. B* **40**, 5411 (1989).
- ⁶M. L. Roukes, M. R. Freeman, R. S. Germain, R. C. Richardson, and M. B. Ketchen, *Phys. Rev. Lett.* **55**, 422 (1985).
- ⁷R. A. Lee and W. N. Wybourne, *J. Phys. F: Met. Phys.* **16**, L169 (1986).
- ⁸K. S. Il'in, N. G. Pitsina, A. V. Sergeev, G. N. Gol'tsman, E. M. Gershenson, B. S. Karasik, E. V. Pechen, and S. I. Krasnovobodtsev, *Phys. Rev. B* **57**, 15623 (1998).
- ⁹R. L. Kautz, G. Zimmerli, and J. M. Martinis, *J. Appl. Phys.* **73**, 2386 (1993).
- ¹⁰P. M. Echternach, M. R. Thoman, C. M. Gould, and H. M. Bozler, *Phys. Rev. B* **46**, 10339 (1992).
- ¹¹F. C. Wellstood, C. Urbina, and J. Clarke, *Phys. Rev. B* **49**, 5942 (1994).
- ¹²V. T. Dolgoplov, A. A. Shashkin, S. I. Dorozhkin, and E. A. Vydrov, *Sov. Phys. JETP* **62**, 1219 (1986).
- ¹³A. Mittal, R. G. Wheeler, M. W. Keller, D. E. Prober, and R. N. Sacks, *Surf. Sci.* **361/362**, 537 (1996).
- ¹⁴E. Chow, H. P. Wei, S. M. Girvin, W. Jan, and J. E. Cunningham, *Phys. Rev. B* **56**, R1676 (1997).
- ¹⁵A. K. M. Wennberg, S. N. Ytterboe, C. M. Gould, H. M. Bozler, J. Klem, and H. Morkoc, *Phys. Rev. B* **34**, 4409 (1986).
- ¹⁶J. J. Lin, *Physica B* **279**, 191 (2000).
- ¹⁷J. J. Lin and C. Y. Wu, *Europhys. Lett.* **29**, 141 (1995).
- ¹⁸G. Bergmann, W. Wei, Y. Zou, and R. M. Mueller, *Phys. Rev. B* **41**, 7386 (1990).
- ¹⁹C. G. Smith and M. N. Wybourne, *Solid State Commun.* **57**, 411 (1986).
- ²⁰J. F. DiTusa, K. Lin, M. Park, M. S. Isaacson, and J. M. Parpia, *Phys. Rev. Lett.* **68**, 1156 (1992).
- ²¹N. G. Pitsina, G. M. Chulkova, K. S. Il'in, A. V. Sergeev, F. S. Pochinkov, E. M. Gershenson, and M. E. Gershenson, *Phys. Rev. B* **56**, 10089 (1997).
- ²²M. E. Gershenson, D. Gong, T. Sato, B. S. Karasik, and A. V. Sergeev, *Appl. Phys. Lett.* **79**, 2049 (2001).
- ²³C. Y. Wu, W. B. Jian, and J. J. Lin, *Phys. Rev. B* **57**, 11232 (1998).
- ²⁴D. R. Heslinga and T. M. Klapwijk, *Solid State Commun.* **84**, 739 (1992).
- ²⁵J. P. Kauppinen and J. P. Pekola, *Phys. Rev. B* **54**, R8353 (1996).
- ²⁶M. M. Leivo, J. P. Pekola, and D. V. Averin, *Appl. Phys. Lett.* **68**, 1996 (1996).
- ²⁷A. Sergeev and V. Mitin, *Phys. Rev. B* **61**, 6041 (2000).
- ²⁸J. Rammer and A. Schmid, *Phys. Rev. B* **34**, 1352 (1986).
- ²⁹D. J. Thouless, *Phys. Rev. Lett.* **39**, 1167 (1977).
- ³⁰D. V. Anghel, J. P. Pekola, M. M. Leivo, J. K. Suoknuuti, and M. Manninen, *Phys. Rev. Lett.* **81**, 2958 (1998).
- ³¹A. M. Savin, M. Prunnila, P. P. Kivinen, J. P. Pekola, J. Ahopelto, and A. J. Manninen, *Appl. Phys. Lett.* **79**, 1471 (2001).
- ³²M. Prunnila, J. Ahopelto, A. M. Savin, P. P. Kivinen, J. P. Pekola, and A. J. Manninen, *Physica E* **13**, 773 (2002).
- ³³G. S. Kumar, G. Prasad, and R. O. Pohl, *J. Mater. Sci.* **28**, 4261 (1993).
- ³⁴R. T. Syme, M. J. Kelly, and M. Pepper, *J. Phys.: Condens. Matter* **1**, 3375 (1989).